Crystal Structure Theory and Applications, 2013, 2, 132-138
http://dx.doi.org/10.4236/csta.2013.23018 Published Online September 2013 (http://www.scirp.org/journal/csta)

Investigation of Some Structural and Mechanical Properties of $Ba_{0.5}Ca_xSr_{0.5-x}TiO_3$ Ceramics

Lubna M. Sharaf El-Deen, Mohamed H. Badr*, Abdel-Mageed H. Khafagy, Dalia U. Nassar
Physics Department, Faculty of Science, Minufiya University, Shibin El Kom, Egypt
Email: *mhbadr0@hotmail.com

Received June 20, 2013; revised July 22, 2013; accepted August 16, 2013

ABSTRACT

$Ba_{0.5}Ca_xSr_{0.5-x}TiO_3$ (BCST) ceramics, where x = 0, 0.1, 0.2, 0.3 and 0.4, were prepared by the conventional solid state reaction technique. X-ray diffraction (XRD) analysis confirmed the formation of BST perovskite phase structure besides some calcium oxide peaks for samples with high Ca content, x. Scanning electron microscopy (SEM) results confirmed the XRD results, *i.e.*, as x increased, the average grain size decreased. Energy dispersive X-ray (EDX) analysis verified the increase of the amount of Ca element with increasing of its content. Mechanical properties such as ultrasonic attenuation, longitudinal wave velocity, and longitudinal elastic modulus were studied by an ultrasonic pulse echo technique at 2 MHz frequency. Investigations of ceramic microstructures and mechanical properties showed their dependence on composition. Increasing of Ca content resulted in a decrease in bulk density and ultrasonic attenuation and an increase in porosity, velocity, and modulus. High temperature ultrasonic studies showed, in addition to Curie phase transition, three or more relaxation peaks and its origin was investigated.

Keywords: BST Ceramics; BCST Ceramics; Phase Transition; Ultrasonic Attenuation; SEM

1. Introduction

$BaTiO_3$ and $SrTiO_3$ are representatives for ABO_3-type perovskite materials. $BaTiO_3$ is usually a ferroelectric material with Curie temperature of 120˚C. $SrTiO_3$ is a paraelectric one with no ferroelectric phase transition [1]. Nevertheless, the combined production of $BaTiO_3$ and $SrTiO_3$ (*i.e.*, $Ba_{1-x}Sr_xTiO_3$) is a solid solution system between $BaTiO_3$ and $SrTiO_3$. Therefore, $Ba_{1-x}Sr_xTiO_3$ (BST) has the simultaneous advantage of high dielectric constant of $BaTiO_3$ and the structural stability of $SrTiO_3$ [1,2]. These ferroelectric materials have attracted considerable attention owing to their unique properties such as chemical stability, high permittivity, high tunability, and low dielectric losses. Furthermore, BST has shown a great promise in applications, such as phase shifting elements in phased array antennas and as tuning elements in devices operating at microwave frequencies [1,3-9]. In view of their merits, the investigation on BST solid solution is therefore significantly important [1,2,9,10]. Furthermore, the Curie temperature of BST can be controlled by adjusting the Ba/Sr ratio and/or doping ions to substitute for A or B sites in the ABO_3 perovskite systems [11,12].

In $BaTiO_3$ materials, an elastic modulus anomaly and a mechanical loss peak are induced at three phase transitions: cubic-tetragonal (ferroelectric-paraelectric), tetragonal-orthorhombic, and orthorhombic-rhombohedra. Some losses due to relaxation processes have been observed in materials having coarse grains in ferroelectric phase [13]. These relaxations were ascribed to the interaction between domain walls and oxygen vacancies diffusion.

The $Ba_{0.5}Sr_{0.5}TiO_3$ (BST) material exhibits the transition from the ferroelectric state to the paraelectric state below room temperature [14]. In a recent work [15], we have investigated the impact of changing barium content on the mechanical properties (such as elastic modulus, attenuation, and velocity of ultrasonic waves) and Curie transition of $Ba_xSr_{1-x}TiO_3$ ceramics. In this work, we aim to investigate thoroughly the effect of Ca-doping on the structural and mechanical properties of $Ba_{0.5}Ca_xSr_{0.5-x}TiO_3$ (BCST) ceramics with x = 0.0, 0.1, 0.2, 0.3 and 0.4. X-ray diffraction, SEM, EDX, and ultrasonic techniques (at a frequency of 2 MHz) were also used to characterize the structure and phase transitions of these ceramics.

2. Materials and Methods

Calcium-doped ceramics with the chemical formula

*Corresponding author.

$Ba_{0.5}Ca_xSr_{0.5-x}TiO_3$ (BCST), where x = 0.0, 0.1, 0.2, 0.3, and 0.4, were prepared by the conventional solid state reaction technique according to the following reaction:

$$(0.5)BaCO_3 + (0.5-x)SrCO_3 + (x)CaO + TiO_2 \rightarrow Ba_{0.5}Ca_xSr_{0.5-x}TiO_3 + (1-x)CO_2 \uparrow$$

For all prepared samples, the reagent grade chemicals of high purity (99.99%) $BaCO_3$, $SrCO_3$, CaO and TiO_2 powders were used as the raw materials and weighed according to the above indicated compositions.

The raw materials were weighed and mixed in the appropriate ratios. Mixtures of required ceramics were first ground thoroughly by a ball milling for 4 h to insure homogeneity. Then, they were calcined at 1100˚C for 11 h in alumina crucibles opened to the air. The calcined compositions were again ground for 6 h. The produced fine calcinated powders were pressed into disc-shaped pellets with 10mm in diameter and 0.6 ~ 1.5 mm in thickness at an iso-static pressure of 5 tons with polyethylene glycol $[(C_2H_4O)_n.H_2O]$ as an organic binder with 2.0% of the weight of the sample. The pelletized samples were finally sintered at 1250˚C for 6h.

The bulk density of ceramics was measured by the conventional Archimedean method. X-ray diffraction (XRD) patterns were recorded with Bruker AXS X-ray diffractometer (D8 Advance) using Cu Kα radiation. The two SEM and EDX measurements were made on JEOL scanning electron microscope (JXA-840A Electron Probe Microanalyzer, INCA x-sight, Oxford Instruments) for the elemental analysis and chemical characterization of the samples. Attenuation of ultrasonic waves (α), longitudinal velocity of wave propagation (V_L), and the longitudinal elastic modulus (L) of tested ceramics were determined by employing the conventional pulse-echo technique at room temperature and during heating as has been reported elsewhere [15].

3. Results

The Archimedean bulk density (ρ_{exp}) and the theoretical density (ρ_x) from the X-ray diffraction patterns of BCST prepared samples were used to calculate the percentage porosity (**Table 1**) according to the equation % porosity = $(\rho_x - \rho_{exp})/\rho_x$ [16]. **Figure 1** shows variations of both the bulk density and porosity of prepared BCST ceramics with the Ca content x where $0.0 \le x \le 0.4$. This figure revealed a linear decease in the density from 4803 to 4339 kg/m^3 as x increased from 0 to 0.4, in harmony with previously reported results [17-19]. Whereas, the percent porosity has increased linearly from 13.4% to 16.5%, for the same variation in Ca content.

Figure 2 shows the room temperature X-ray diffract-graphs for all tested BCST ceramics between 20˚ and 80˚. The intensity of peaks for different values of Ca content, x, were normalized and shifted for clarity pur-

Table 1. The variation of the density (bulk density, ρ_{exp}, and theoretical density, ρ_x) the percent porosity, the ultrasonic attenuation, longitudinal velocity, modulus, and lattice parameter of BCST ceramics with different values of Ca content, x.

Ca	Density		Porosity	Attenuation	Long.	Long. Elastic	Lattice
cont.	ρ_{exp}	ρ_x	(%)	α	Velocity	Modulus	Parameter
x	(kg/m^3)	(kg/m^3)	(dB/cm)	V_L (m/s)	L(GPa)		a (Å)
0.0	4803	5509	13.423	24.261	1316.1	8.314	3.9510
0.1	4748	5601	13.650	19.983	1642.5	12.815	3.9461
0.2	4521	5491	15.157	16.945	1873.9	15.872	3.9415
0.3	4483	5481	16.168	15.678	2012.9	18.152	3.9368
0.4	4339	5375	16.535	13.482	2167.2	20.384	3.9325

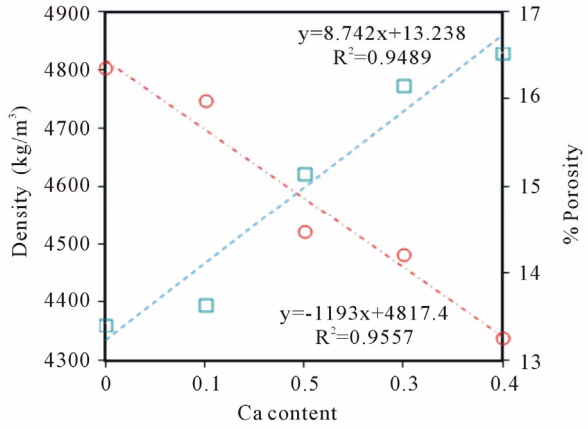

Figure 1. Variation of the density and porosity with the Ca content of $Ba_{0.5}Ca_xSr_{0.5-x}TiO_3$ ceramics sintered at 1250˚C for 6 h.

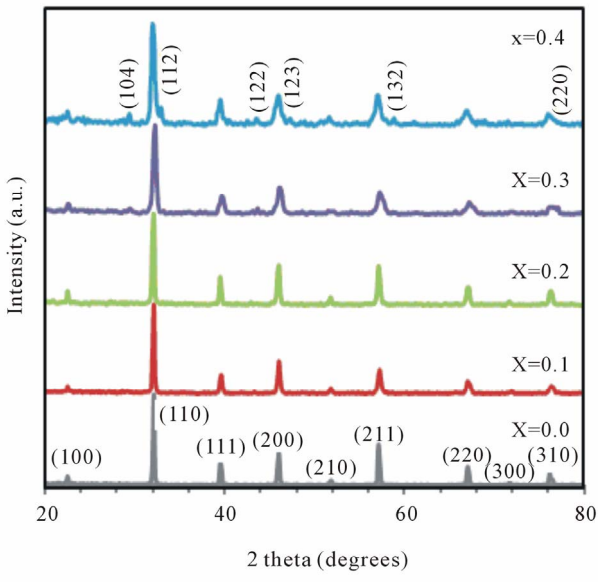

Figure 2. XRD patterns of $B_{0.5}Ca_xSr_{0.5-x}TiO_3$ (BCST) ceramics with Ca content x = 0.0, 0.1, 0.2, 0.3 and 0.4.

poses. All peaks were indexed in the cubic structure due to their observed reflections of different polycrystalline orientations [20-22] as indicated by the (110) index; the major peak of highest intensity. Variation of the lattice parameter a (Å) with different Ca content was listed in **Table 1**.

The chemical compositions of tested BCST ceramics were determined from EDX spectra and listed in **Table 2**. The scanning electron microscopy (SEM) is a powerful experimental technique to determine the particle size, pore concentration, and inclusions in a material. **Figures 3(a)-(d)** show the scanning electron micrographs taken at room temperature of BCST ceramics with Ca content in the range $0.0 \leq x \leq 0.4$. The SEM for x = 0.2 was not included in this figure for brevity reasons. These micrographs describe the surface property of samples, microstructure, size, and distribution of particles. Whereas, the average grain size dependence (as determined from XRD and SEM investigations) on the Ca content was illustrated in **Figure 4**.

Figure 5 shows the regression line which illustrates the variation of ultrasonic attenuation (α) of ultrasonic waves, measured at room temperature, with the Ca content of the prepared $Ba_{0.5}CaSr_{0.5-x}TiO_3$ ceramics sintered at 1250˚C for 6 h. Inspection of the figure reveals that α is dependent on the composition of the tested ceramic, *i.e.*, it is exponentially decreased with increasing of Ca content over the above mentioned investigated range (see also **Table 1**).

Figure 6 shows the dependences of both longitudinal ultrasonic velocity and longitudinal elastic modulus on composition of $Ba_{0.5}Ca_xSr_{0.5-x}TiO_3$ (BCST) ceramics with x= 0.0, 0.1, 0.2, 0.3 and 0.4 were sintered at 1250˚C for 6 h. As could be deduced from this figure, both of the ultrasonic velocity and modulus have increased nonlinearly with the increase in Ca content from 0 to 0.4.

Figures 7(a) and **(b)**, show the variations of ultrasonic attenuation (α) of ultrasonic waves, at 2 MHz frequency, with temperature for $Ba_{0.5}Ca_xSr_{0.5-x}TiO_3$ ceramics sintered at 1250˚C for 6h with x = 0.0, 0.1, 0.4 and x = 0.0, 0.2, 0.3, respectively. The figures reveal well-defined damping peaks at 266˚C, 313˚C, 319˚C, 325˚C and

Table 2. Initial Ca contents and EDX analyses results for the investigated BCST ceramics.

Ca cont., x	EDX analyses results (wt.%)	EDX Sr/Ca
0.0	$Ba_{0.551}Sr_{0.500}Ti_{1.121}O_3$	--
0.1	$Ba_{0.577}Ca_{0.015}Sr_{0.407}Ti_{1.173}O_3$	27.97
0.2	$Ba_{0.593}Ca_{0.151}Sr_{0.370}Ti_{1.058}O_3$	2.50
0.3	$Ba_{0.588}Ca_{0.256}Sr_{0.370}Ti_{0.979}O_3$	1.42
0.4	$Ba_{0.590}Ca_{0.327}Sr_{0.198}Ti_{1.057}O_3$	0.61

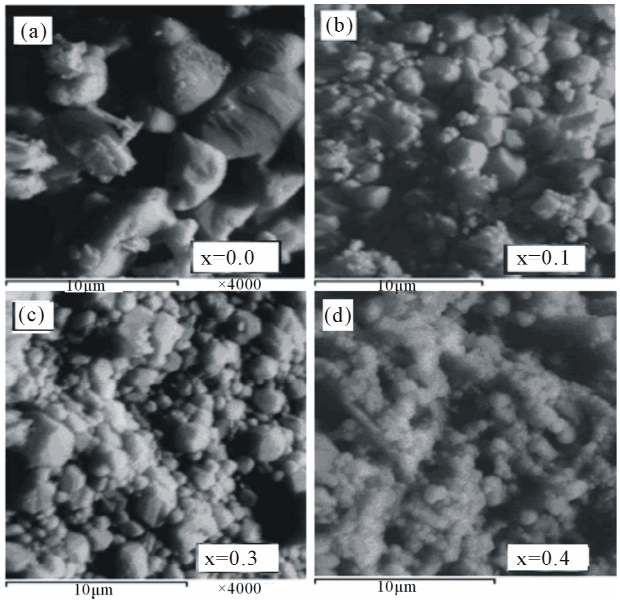

Figure 3. SEM micrographs of $Ba_{0.5}Ca_xSr_{0.5-x}TiO_3$ ceramics. The bars represent 10 μm in length.

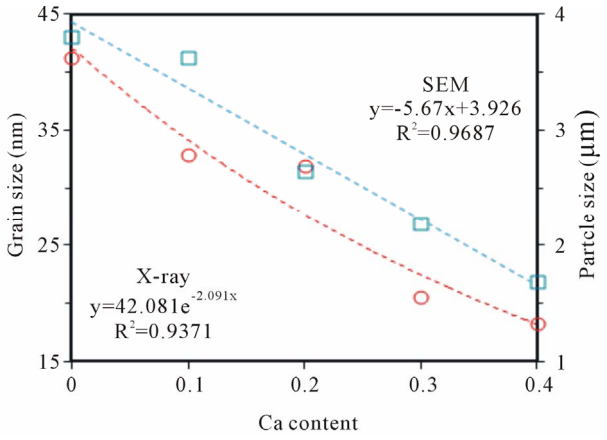

Figure 4. The dependence of average grain size and particle size on the Ca content, x, for BCST ceramics.

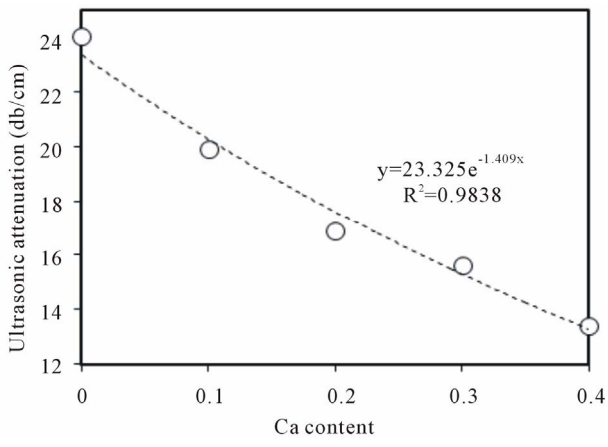

Figure 5. Variation of the ultrasonic attenuation with Ca content in BCST ceramics sintered at 1250˚C for 6 h.

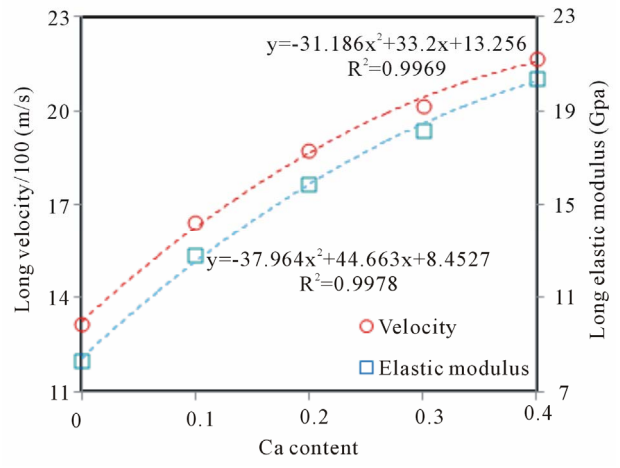

Figure 6. Variation of longitudinal ultrasonic velocity and longitudinal elastic modulus with the Ca content of BCST ceramics sintered at 1250˚C for 6 hr.

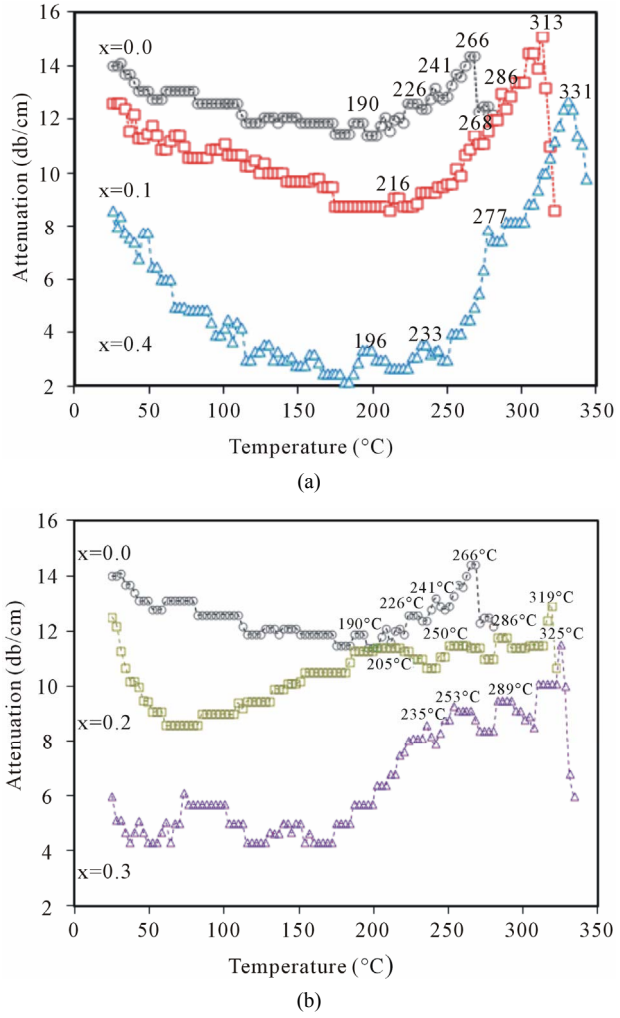

Figure 7. (a): Variation of ultrasonic attenuation with temperature at 2 MHz for x = 0, 0.1 and 0.4; (b): Variation of ultrasonic attenuation with temperature at 2 MHz for with x = 0, 0.2 and 0.3.

331˚C for all tested specimens of x = 0.0, 0.1, 0.2, 0.3 and 0.4, respectively. Also, a shoulder was observed for each ceramic near the room temperature. However, locations and shapes of all observed peaks and shoulders depend on the composition of ceramics.

4. Discussion

4.1. Density and Porosity

The observed decrease of the density of tested BCST ceramics (**Figure 1**) is attributed to: 1) distortion occurred due to substitution of Ca atoms of lower atomic weight (40.08 a.m.u.) with Sr ones of higher atomic weight (87.62 a.m.u.) in the (BCST) ceramics [17-19]; and 2) the observed increase in the percent porosity which is attributed to substitution of Ca atoms of lower ionic radius (0.99 Å) with Sr ones of higher ionic radius (1.12 Å) [18] (see **Table 1**).

4.2. XRD, SEM and EDX

XRD patterns, illustrated in **Figure 2**, showed all major X-ray peaks of diffraction for BCST ceramics. The patterns confirm the formation of perovskite phase of BST ceramics obtained previously in [16,20-22]. Also, these XRD patterns showed a cubic perovskite phase which confirmed that Ca^{+2} ions substitution for Sr^{+2} can be mostly incorporated into the perovskite structure of BST material. Moreover, as the Ca content increased (x = 0.3 and 0.4) very small assigned peaks were observed and indexed to their corresponding orientations as shown on x = 0.4 pattern, **Figure 2**. The intensity of these subsidiary peaks slightly increased for x = 0.4 and were attributed to the secondary phase of calcium oxide in these ceramics. The lattice parameter a for the polycrystalline cubic phase was calculated from the $d_{(hkl)}$ and 2θ degrees values, and typical values were listed in **Table 1**. As could be seen from **Figure 2**, the samples with $x \leq 0.2$ showed no apparent changes in the relative intensities and broadening of peaks. This suggested x = 0.2 sets the limit of the salability range when Ca substitutes Sr in BST ceramics sintered at 1250˚C for 6 h for the studied values of x. As Ca content increases (x = 0.3 and 0.4) the peaks become broadened to some extent in addition to calcium oxide peaks. The previous observations indicate that increasing the content of Ca in the BCST materials decreases the particle size, lattice parameter a (Å), and volume of unit cell a^3 (Å^3) when Sr^{2+} is partly substituted with Ca^{2+}, which is consistent with the fact that the radius of Ca^{2+} ion is smaller than that of Sr^{2+} ions [19], see also **Table 1**.

Referring to EDX analysis results tabulated in **Table 2**, the x = 0.0 sample consists of Ti, Ba and Sr, *i.e.*, it is Ca-free sample. Whereas for x > 0.0 samples, EDX results confirm the presence of Ca in addition to the Ti, Ba,

and Sr elements. Also, it is clear to note the decrease in intensity of strontium in the final products with increasing Ca content than that of the initial reactants. For the above tested specimens, the wt.% of each of these elements, as deduced from EDX analysis given in **Table 2**, indicates that the amount of Ca element in the sample increases depending on increasing Ca incorporation in the $B_{0.5}Ca_xSr_{0.5-x}TiO_3$ ceramics.

It is evident that the Sr/Ca ratio of BCST samples resulted from EDX analysis are different from that in the initial reactants compositions. Regardless of these differences the trends of Sr/Ca ratios in the two cases are the same, *i.e.*, the Sr/Ca ratio decreases as the x value increases, and the Sr/Ca ratios from EDX analyses are consistently smaller than that in the initial reaction system. Consequently, Ca incorporation has its effect on the mechanical and electrical properties of tested ceramics as will be discussed later on in the following sections.

Figure 3(a) reveals that the average particle size is about 6.77 μm for $Ba_{0.5}Sr_{0.5}TiO_3$ (BST) ceramic which is bigger than that of BCST ceramics in **Figures 3(b)-(e)** doped with Ca. This is in agreement with the work of [23] in which BST with x = 0.5 sample sintered at 1260˚C showed a large distribution of grain dimensions between 5 and 25 μm. Sub-micronic grains ≈ 0.90 μm, are located at the boundary of the largest ones as observed by [24]. Also, a less homogeneous microstructure, with an evident bi-modal grain size distribution was pointed out by the SEM images (**Figures 3(b)-(e)**). Besides, large particles, exaggerated smaller grains resulted by abnormal grain growth, were also noticed. The average values of particle size of studied ceramics, shown in **Figure 4**, were calculated from the micrographs of **Figure 3** according to the selected intersected lines method [25]. However, the average particle size values which found from ESM micrographs were decreased from 3.81 μm to 1.69 μm with increasing of Ca content in the sample from x = 0.0 to x = 0.4, which are larger than those values obtained for these grains as calculated by using Scherrer's equation (see **Figure 4**). The dependence of grain size on Ca content, **Figure 4**, seems to be decreased for both values determined from the X-ray and the SEM measurements. In other words, as the calcium content, x, increases in the ceramic from 0 to 0.4, the grain size is decreased in consistent with the A-site cation size effect reported in previous literature [18,19].

4.3. Mechanical Properties Investigations

4.3.1. Room Temperature Characterization

The observed decrease in the ultrasonic attenuation (**Figure 5**) may be attributed to the observed decrease in the crystallites or grain sizes associated with the replacement of Sr by Ca in BCST ceramics, as seen in **Figure 4**. This view agrees with our XRD and SEM investigations and in harmony with previous results [18,19,26].

4.3.2. Ultrasonic Velocity and Elastic Modulus

Variations of both the ultrasonic velocity and longitudinal elastic modulus, **Figure 6**, could be understood based on the effect of Ca content on microstructures of these ceramics. We have shown that the increase in Ca content in the ceramics decreases the grain or particles sizes due to its insertion in A-sites with its smaller radius as observed from X-ray results and SEM micrographs (see **Figure 4**). This decrease in grain size is known to raise the velocity of wave propagation [15,26]. Therefore, the observed increase in velocity is attributed to the decrease in grain sizes in the ceramics' microstructures with the increase in Ca content inside the samples. Also, it is known that the elastic modulus is proportional to the velocity squared according to the equation $L = V^2\rho$. Even though the density decreases with increasing calcium content, the increase in L with the increase in the wave velocity (V) overwhelms the density effect due to the velocity squared character.

4.3.3. Temperature Dependence of Ultrasonic Attenuation

Variation of ultrasonic attenuation (α) with temperature, shown in **Figures 7(a)** and **(b)**, could be interpreted in terms of the effect of Ca doping in tested BCST ceramics. It has been noticed that the observed damping peaks were found to be dependent on the composition. Explicitly, each peak position shifts to higher temperatures with a reduction in its maximum and the peak shape becomes broadened and diffused, especially in the ferroelectric side, as Ca replaces Sr in BCST ceramics. These observations are in good agreement with previously reported investigations of dielectric constant in $Ba_{1-2x}Sr_xCa_xTiO_3$ ceramics [18]. The sample with x = 0.0 (calcium-free sample, **Figure 7**) has the lowest Curie temperature (T_C) and occurred at 266˚C. As the calcium content increases at the expense of strontium content, T_C increases, namely, for BCST with x = 0.1, 0.2, and 0.3 the Curie temperature T_C = 313, 319, and 325˚C, respectively. Furthermore, for the highest calcium content with x = 0.4, T_C occurred at the highest Curie temperature of 331˚C. Therefore, it can be said that, on replacing Sr by Ca the peak temperature of the Curie transition shifts to higher temperatures which is in good agreement with previous results [18,19,26]. However, their occurrence in this range of higher temperatures, may be due to the high operated ultrasonic frequency (2 MHz) and perhaps also to the effect of electric field produced on the ceramic surfaces during these measurements (since tested samples were spring-loaded in the holder as well as these ferroelectric materials are pyroelectric and piezoelectric). This induced electric field can preserve the ordered states in ferroelectric domains for more time, in the ferroelectric phase, in the manner that it needs—in addition to the applied ultrasonic energy—more thermal heat which in turn

raises the temperature of order-disorder temperature phase transition or the Curie temperature. However, this needs more investigations which will be considered in future work on these ferroelectric materials.

The above conclusion may be summed in another way as follows: when the Ca content increases at the expenses of the Sr in the investigated range, the average grains size decreases (as seen from X-ray measurements, and SEM images) and seen in **Figure 4**. Therefore, the ceramic becomes to some extent more rigid, in addition to the effect of the electric field induced due to both the piezoelectric (direct and indirect) and the pyroelectric effects, which allows the ceramic to require more thermal energy for its disorder state to be attained through the Curie transition, thus the increase in the transition temperature from 266˚C to 331˚C as obtained. Also, the observed shoulders on the plots of all ceramics in **Figures 7(a)** and **(b)** refer to the high temperature wings of the orthorhombic to tetragonal phase transition in each tested BCST ceramic which seems to occur around 0˚C temperature [26-28].

Regarding the relaxation peaks observed below the structural phase transition (T_C) in the ferroelectric regions, there are three (or more) relaxation peaks on each plot in the ultrasonic attenuation-temperature spectra BCST ceramics (see **Figures 7(a)** and **(b)**) whose heights and positions are composition dependent. All of these relaxation peaks can be described by a thermal activated Arrhenius relationship [29] and their origin could be understood according to their values of activation energy as has been done in the case of BST ceramics in published work [15,26]. Anyhow, the calculated values of activation energy (W) of these relaxation processes were listed in **Table 3**. Referring to the table, it can be observed that the calculated values for activation energies of relaxation peaks corresponding to each tested ceramic are dependent on their origin. Namely, it could be attributed to diffusion of point defects in the ferroelectric phase [26, 27-29] as occurred in the first relaxation (W is larger than 1.1 eV) and to diffusion of oxygen vacancies associated to domain walls and domain wall motions as occurred in the second and third relaxations when W is less than 1.1 eV, respectively [26-28]. Besides, it is also observed from **Table 3** that, for each relaxation, both of the activation energy value and position increased and decreased with the gradual increase in Ca content overall the tested range from x = 0.0 to x = 0.4.

Table 3. Temperatures and activation energies of relaxation peaks occurred in BCST ceramics, sintered at 1250˚C for 6 h, with different Ca contents, x.

Ca	1st Relax.		2nd Relax.		3rd Relax.	
content,	T	W	T	W	T	W
x	(˚C)	(eV)	(˚C)	(eV)	(˚C)	(eV)
0.0	190	1.209	226	1.051	241	1.002
0.1	216	1.088	268	0.929	286	0.890
0.2	205	1.135	250	0.976	286	0.890
0.3	235	1.020	253	0.967	289	0.884
0.4	196	1.175	233	1.027	277	0.909

5. Conclusion

In this work, $Ba_{0.5}Ca_xSr_{1-x}TiO_3$ ceramics with x = 0.0, 0.1, 0.2, 0.3 and 0.4 were prepared by solid state reaction technique and studied by XRD, SEM, EDX, and ultrasonic techniques. XRD data confirmed the formation of the perovskite phase structure in addition to peaks observed for some tested ceramics which have been related to excess Ca contents in doped samples. SEM images and EDX analysis confirmed the appearance of the major perovskite phase and an increase of Ca ions upon increasing its content. The effect of increasing of Ca content in BCST samples resulted in a decrease of particle size, as confirmed by XRD and SEM images. Also, BCST ceramics showed composition dependence for their density, longitudinal velocity, elastic modulus, and attenuation upon increasing Ca content (from x = 0 to 0.4) and resulted in a decrease of bulk density, and ultrasonic attenuation, and an increase in velocity, and longitudinal modulus. The temperature dependence of ultrasonic attenuation investigations for BCST samples have revealed, the occurrence of not only, the Curie (or tetragonal to cubic) transition and the right shoulder of (orthorhombic to tetragonal) transition, but also some relaxation peaks associated with point defects and diffusion of oxygen vacancies. However, the curie transition temperature T_C showed to be dependent on the content of Ca; its increasing resulted in an increase in T_C of the tested BCST samples.

REFERENCES

[1] K. Abe and S. Komatsu, "Ferroelectric Properties in Epitaxially Grown $Ba_xSr_{1-x}TiO_3$ Thin Films," *Journal of Applied Physics*, Vol. 77, No. 12, 1995, pp. 6461-6465. doi:10.1063/1.359120

[2] Z. L. Wang and Z. C. Kang, "Functional and Smart Materials—Structural Evolution and Structural Analysis," Science Press, Beijing, 2002.

[3] L. C. Sengupta and S. Sengupta, "Novel Ferroelectric Materials for Phased Array Antennas," *IEEE Transactions on Ultrasonics*, *Ferroelectrics*, *and Frequency Control*, Vol. 44, No. 4, 1997, pp. 792-797. doi:10.1109/58.655193

[4] S. S. Gevorgian and E. L. Kollberg, "Do We Really Need Ferroelectrics in Paraelectric Phase Only in Electrically Controlled Microwave Devices?" *IEEE Transactions on Microwave Theory and Techniques*, Vol. 49, No. 11, 2001, pp. 2117-2124. doi:10.1109/22.963146

[5] P. C. Joshi and M. W. Cole, "Mg-doped $Ba_{0.6}Sr_{0.4}TiO_3$ Thin Films for Tunable Microwave Applications," *Ap-*

plied Physics Letters, Vol. 77, No. 2, 2000, pp. 289-291. doi:10.1063/1.126953

[6] W. Chang and L. Sengupta, "MgO-mixed Ba0.6Sr0.4TiO3 Bulk Ceramics and Thin Films for Tunable Microwave Applications," *Journal of Applied Physics*, Vol. 92, No. 7, 2002, pp. 3941-3946. doi:10.1063/1.1505669

[7] M. Kuwabara, H. Matsuda and Y. Ohba, "Varistor Characteristics in PTCR-Type (Ba,Sr)TiO_3 Ceramics Prepared by Single-Step Firing in Air," *Journal of Materials Science*, Vol. 34, No. 11, 1999, pp. 2635-2639. doi:10.1023/A:1004661018287

[8] J. F. Scott, M. Azuma, E. Fujii, T. Otsuki, G. Kano, M. C. Scott, C. A. Paz de Araujo, L. D. McMillan and T. Roberts, "Microstructure-Induced Schottky Barrier Effects in Barium Strontium Titanate (BST) Thin Films for 16 and 64 Mbit (DRAM cells)," *Proceedings of International Symposium on Integrated Ferroelectrics*, New York, 1992, p. 356.

[9] X. Weidong, L. Yanrong and Y. Chun, "First Principle Studies on Fine Structure for $Ba_xSr_{1-x}TiO_3$," *Chinese Journal of Chemical Physics*, Vol. 18, No. 2, 2005, pp. 179-182.

[10] T. Hu, H. Jantunen, A. Uusimaki and S. J. Leppavuori, "BST Powder with Sol-Gel Process in Tape Casting and Firing," *Journal of the European Ceramic Society*, Vol. 24, No. 6, 2004, pp. 1111-1116. doi:10.1016/S0955-2219(03)00427-8

[11] V. V. Lemanov, "Concentration Dependence of Phonon Mode Frequencies and the GrüNeisen Coefficients in BaxSr$_{1-x}$TiO3 Solid Solutions," *Physics of the Solid State*, Vol. 39, No. 2, 1997, pp. 318-322. doi:10.1134/1.1129842

[12] B. Jaffe, W. R. Cook and H. Jaffe, "Piezoelectric Ceramics," Academic Press, London, 1971.

[13] B. L. Cheng, M. Gabbay, M. Maglione and G. Fantozzi, "Relaxation Motion and Possible Memory of Domain Structures in Barium Titanate Ceramics Studied by Mechanical and Dielectric Losses," *Journal of Electroceramics*, Vol. 10, No. 1, 2003, pp. 5-18. doi:10.1023/A:1024007407033

[14] A. Ioachim, M. I. Toacsan, M. G. Banciu, L. Nedelcu, C. Plapcianu, H. V. Alexandru, C. Berbecaru, D. Ghetu, G. Stoica and R. Ramer, "Frequency Agile BST Materials for Microwave Applications," *Journal of Optoelectronics and Advanced Materials*, Vol. 5, No. 5, 2003, pp. 1389-1393.

[15] M. H. Badr, L. M. Sharaf El-Deen, A. H. Khafagy and D. U. Nassar, "Structural and Mechanical Properties Characterization of Barium Strontium Titanate (BST) Ceramics," *Journal of Electroceramics*, Vol. 27, No. 3-4, 2011, pp. 189-196. doi:10.1007/s10832-011-9664-5

[16] O. P. Thakur, C. Prakash and D. K. Agrawal, "Dielectric Behavior of $Ba_{0.95}Sr_{0.05}TiO_3$ Ceramics Sintered by Microwave," *Materials Science and Engineering*: *B*, Vol. 96, No. 3, 2002, pp. 221-225. doi:10.1016/S0921-5107(02)00159-9

[17] J. F. Scott, "High-Dielectric Constant Thin Films for Dynamic Random Access Memories (DRAM)," *Annual Review of Materials Research*, Vol. 28, No. 1, 1998, pp. 79-100. doi:10.1146/annurev.matsci.28.1.79

[18] C. Berbecaru, H. V. Alexandru, C. Porosnicu, A. Velea, , A. Ioachim, L.Nedelcu and M. Toacsan, "Ceramic Materials $Ba_{(1-x)}Sr_xTiO_3$ for Electronics—Synthesis and Characterization," *Thin Solid Films*, Vol. 516, No. 22, 2008, pp. 8210-8214. doi:10.1016/j.tsf.2008.04.031

[19] S. Yun, X. Wang, B. Li and D. Xu, "Dielectric Properties Ca-Substituted Barium Strontium Titanate Ferroelectric Ceramics," *Solid State Communications*, Vol. 143, No. 10, 2007, pp. 461-465. doi:10.1016/j.ssc.2007.06.031

[20] V. V. Lemanov, A. V. Sotnikov, E. P. Smirnova, P. P. Syrnikov and E. A. Tarakanov, "Phase Transitions and Glasslike Behavior in $Sr_{(1-x)}Ba_xTiO_3$," *Physical Review B*, Vol. 54, No. 5, 1996, pp. 3151-3157. doi:10.1103/PhysRevB.54.3151

[21] A. K. Singh, Subrat K. Barik, R. N. P. Choudhary and P. K. Mahapatra, "Ac Conductivity and Relaxation Mechanism in $Ba_{0.9}Sr_{0.1}TiO_3$," *Journal of Alloys and Compounds*, Vol. 479, No. 1-2, 2009, pp. 39-42. doi:10.1016/j.jallcom.2008.12.130

[22] Y.-C. Liou and C.-T. Wu, "Synthesis and Diffused Phase Transition of $Ba_{0.7}Sr_{0.3}TiO_3$ Ceramics by a Reaction-Sintering Process," *Ceramics International*, Vol. 34, No. 3, 2008, pp. 517-522. doi:10.1016/j.ceramint.2006.11.005

[23] C. Fu, C. Yang, H. Chen, W. Wang, and L. Hu, "Microstructure and Dielectric Properties of $Ba_xSr_{1-x}TiO_3$ Ceramics," *Materials Science and Engineering*: *B*, Vol. 119, No. 2, 2005, pp. 185-188. doi:10.1016/j.mseb.2005.02.056

[24] A. Ioachim, R. Ramer, M. I. Toacsan, M. G. Banciu, L. Nedelcu, C. A. Dutu, F. Vasiliu, H. V. Alexandru, C. Berbecaru, G. Stoica and P. Nita, "Effect of the Sintering Temperature on the Ba(Zn 1/3Ta 2/3)O3 Dielectric Properties," *Journal of the European Ceramic Society*, Vol. 27, No. 2-3, 2007, pp. 1117-1122. doi:10.1016/j.jeurceramsoc.2006.05.023

[25] A. Ioachim, H. V. Alexandru, C. Berbecaru, S. Antohe, F. Stanculescu, M. G. Banciu, M. I. Toacsan, L. Nedelcu, D. Ghetu, A. Dutu and G. Stoica, "Dopant Influence on BST Ferroelectric Solid Solutions Family," *Materials Science and Engineering*: *C*, Vol. 26, No. 5-7, 2006, pp. 1156-1161. doi:10.1016/j.msec.2005.09.045

[26] G. Cigna, "Dynamic Mechanical Properties, Struc- ture, and Composition of Impact Polystyrene," *Journal of Applied Polymer Science*, Vol. 14, No. 7, 1970, pp. 1781-1793. doi:10.1002/app.1970.070140712

[27] H. Frayssignes, B. L. Cheng, G. Fantozzi and T. W. Button, "Phase Transformation in BST Ceramics Investigated by Internal Friction Measurements," *Journal of the European Ceramic Society*, Vol. 25, No. 13, 2005, pp. 3203-3206. doi:10.1016/j.jeurceramsoc.2004.07.030

[28] B. L. Cheng, B. Su, J. E. Holmes, T. W. Button, M. Gabbay and G. Fantozzi, "Dielectric and Mechanical Losses in (Ba,Sr)TiO_3 Systems," *Journal of Electroceramics*, Vol. 9, No. 1, 2002, pp. 17-23. doi:10.1023/A:1021633917071

[29] A. S. Nowick and B. S. Berry, "Anelastic Relaxation in Crystalline Solids," Academic Press, New York, 1972.

